Published by :
https://www.ijert.org/
An International Peer-Reviewed Journal

International Journal of Engineering Research & Technology (IJERT)
ISSN: 2278-0181
Vol. 15 Issue 07 , July - 2026

Neural Network-Based Phase Correction for RIS-Assisted mmWave 5G NR Links

Ghulam Muhayy ud Din Qureshi[1], Tahir Hussain Nazir Hussain[2], Fayaz Muhammad Mufti[3]
Saudi Telecom Operator

***Abstract*—Millimeter-wave (mmWave) 5G New Radio (NR) can provide wide bandwidth and multi-gigabit data rates; however, its high sensitivity to physical blockage significantly restricts coverage, particularly when a direct line-of-sight (LoS) path is unavailable. Reconfigurable Intelligent Surfaces (RISs) offer a promising solution by redirecting radio signals around obstacles through controlled passive reflections. Their effectiveness, however, depends on accurately configuring the phase shift of each RIS element, which requires reliable channel state information (CSI). Acquiring such information becomes increasingly complex and resource-intensive as the number of RIS elements grows.**

This paper presents a physically grounded simulation of an RIS-assisted mmWave communication link operating at 26 GHz. Unlike conventional approaches that model angle estimation errors as simple additive noise, the proposed model introduces realistic nonlinear bias into the angle-of-departure (AoD) estimate used for RIS phase configuration. A feed-forward neural network is trained to compensate for this bias using noisy angle and distance measurements. Its performance is evaluated against an uncorrected baseline and a linear-regression-based correction method under 1-bit, 2-bit, and 3-bit RIS phase-shifter quantization.

Simulation results indicate that naive phase configuration can reduce the achievable beamforming gain by approximately 20 dB compared with the ideal configuration. Linear regression recovers a substantial portion of this loss, while the neural-network-based approach delivers a further and consistent improvement, particularly under coarse 1-bit phase quantization. The findings demonstrate the potential of machine-learning-assisted phase configuration to improve RIS-enabled mmWave coverage in obstacle-dense environments. The paper also discusses the limitations of simulation-based evaluation and identifies future work involving validation with real-world channel measurements.

***Index Terms*—5G NR, millimeter wave, reconfigurable intelligent surface, machine learning, phase configuration, beamforming, channel state information, coverage enhancement.**

I. Introduction

Millimeter-wave (mmWave) spectrum, typically defined from 24 GHz to 300 GHz, provides the wide contiguous bandwidth required to support multi-gigabit 5G NR services. However, these high-frequency signals experience severe propagation limitations. Free-space path loss is considerably higher than at lower frequencies, diffraction around obstacles is weak, and common construction materials can introduce tens of decibels of additional attenuation. As a result, even a single obstruction between the gNB and the UE can degrade a high-capacity mmWave connection into a weak or completely unavailable link.

For this reason, mmWave coverage depends heavily on maintaining a clear line-of-sight path. Ensuring such a path is particularly challenging in dense urban areas and mass-gathering environments, where buildings, temporary structures, vehicles, and even moving crowds can frequently block the radio signal. Reconfigurable Intelligent Surfaces (RIS) have emerged as a potential solution to this coverage challenge. An RIS consists of a passive panel containing many small reflective elements, each capable of independently adjusting the phase of an incident electromagnetic wave. When installed on a building façade, wall, or other suitable structure, the surface can redirect signal energy around an obstruction and toward a UE located within a coverage shadow.

The practical benefit of RIS, however, is highly dependent on accurate configuration. The phase shift applied by each element must be carefully selected so that all reflected signal components arrive coherently at the receiver. This requires reliable knowledge of the signal's angle of incidence and the required reflection direction toward the UE.

Accurate RIS configuration requires precise knowledge of both the angle of incidence and the angle of departure. In practical deployments, however, these angular parameters must be estimated from noisy and imperfect channel measurements. Even small estimation errors can produce incorrect phase assignments across the RIS elements, preventing coherent signal combination at the receiver and significantly reducing the theoretical beamforming gain.

This study is also motivated by the broader digital-infrastructure objectives of Saudi Arabia's Vision 2030 [1]. Within this context, mmWave spectrum is being considered as an additional capacity layer for dense urban areas and high-demand event environments. RIS-assisted coverage extension may help make such deployments more practical by improving service in obstructed locations without requiring a prohibitively dense deployment of additional small cells.

Based on this motivation, the remainder of this paper develops a physically grounded model of RIS phase-configuration errors under realistic angle-estimation conditions. A neural-network model is then trained to predict and correct the resulting phase errors. Its performance is evaluated in terms of beamforming gain and compared with both an uncorrected RIS configuration and a linear-regression baseline. The evaluation is conducted across multiple RIS phase-quantization resolutions to assess the robustness of the proposed approach under realistic hardware constraints.

II. Background and Related Work

Reconfigurable Intelligent Surfaces have been widely proposed as a key enabling technology for future smart radio environments. Unlike conventional relays or repeaters, RIS

International Journal of Engineering Research & Technology (IJERT)
ISSN: 2278-0181
Vol. 15 Issue 07 , July - 2026

technology seeks to reshape the wireless propagation environment itself by controlling how incident electromagnetic waves are reflected toward intended receivers [5]–[7].

The RIS propagation framework adopted in this study is based on the path-loss and channel models presented by Tang et al. [3] and Danufane et al. [4]. Tang et al. developed and experimentally validated a path-loss model for RIS-assisted mmWave communication links, while Danufane et al. provided a rigorous electromagnetic interpretation of RIS-assisted propagation using Green's theorem. These studies show that, when the reflected components are coherently aligned, the array gain of an N-element RIS increases favorably with the number of reflecting elements. Consequently, even moderately sized RIS panels can provide meaningful coverage improvement, provided that their phase responses are configured accurately.

Practical RIS hardware, however, cannot generally provide continuous phase control. Instead, each reflecting element is restricted to a finite number of discrete phase states. The hardware model considered in this paper follows the discrete phase-shift formulation introduced by Wu and Zhang [8], allowing the effect of different phase-quantisation resolutions to be evaluated.

The target use case of this work is the restoration of mmWave coverage when the direct link between the gNB and the UE is blocked. The feasibility of using passive reflecting structures to improve non-line-of-sight mmWave coverage was demonstrated by Khawaja et al. [9]. Their findings support the broader principle that appropriately positioned reflecting surfaces can redirect signal energy into shadowed regions and improve link reliability without requiring an additional active radio node.

The main challenge addressed in this paper is that RIS performance depends directly on the accuracy of the available channel-state and angular information. Since the phase configuration is calculated from estimated propagation parameters, errors in those estimates are translated into element-level phase errors across the surface. These errors reduce coherent combining at the receiver and may significantly diminish the array gain predicted under ideal channel knowledge.

The accuracy of RIS phase configuration is fundamentally limited by the quality of the channel-state information used to determine it. Acquiring complete CSI for a surface containing a large number of elements can introduce substantial training overhead and computational complexity. Consequently, several machine-learning approaches have been proposed to reduce the dependence on explicit CSI estimation and improve RIS configuration under imperfect channel information.

Jiang et al. [12] proposed a learning-based framework for joint reflection and beamforming design using implicit channel estimation, thereby avoiding the need for complete explicit CSI acquisition. Özdogan and Björnson [11] investigated deep-learning-based phase reconfiguration for intelligent reflecting surfaces, demonstrating the potential of neural networks to determine effective reflection patterns directly from channel observations. Peng et al. [10] introduced RISnet, a domain-knowledge-driven neural-network architecture designed to optimise RIS configurations under partial CSI and mutual-coupling effects.

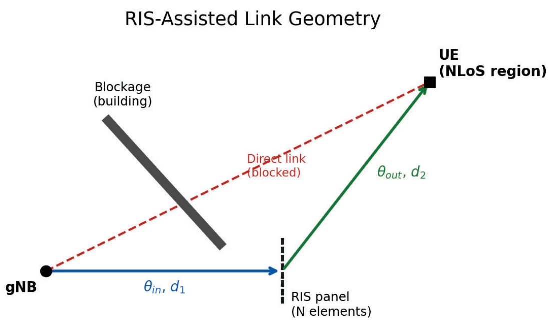

Fig. 1: RIS-assisted link geometry in which the direct path between the gNB and the UE is blocked, while the RIS panel establishes an alternative reflected path characterized by the angle of incidence, θ_{in}, and the angle of departure, θ_{out}.

The work most closely related to the present study is that of Fondo-Ferreiro et al. [13], who trained a fully connected neural network to estimate the optimal RIS phase-shift profile from noisy CSI measurements. Their approach achieved throughput performance within approximately 1% of the optimal solution after correction. A broader review of RIS optimisation methods, ranging from conventional closed-form and iterative techniques to artificial-intelligence-based approaches, is provided by Li et al. [14].

The present work follows the general learning-based direction established in [11] and [13] by training a neural network to recover an effective RIS phase configuration from imperfect angular and channel estimates. However, this study differs in two important aspects. First, it considers a nonlinear, position-dependent estimation-bias pattern that represents multipath-corrupted angle-of-departure estimation, rather than assuming only independent additive noise. Second, the proposed neural-network correction is explicitly compared with a linear-regression baseline. This comparison is intended to isolate the performance improvement attributable specifically to nonlinear modelling and to determine whether the additional complexity of the neural network is justified.

III. Technical Explanation

An RIS-assisted communication link consists of two cascaded propagation segments: the gNB-to-RIS link, which represents the incident path, and the RIS-to-UE link, which represents the reflected path. Fig. 1 illustrates the blocked line-of-sight scenario considered in this study. In this configuration, the direct gNB-to-UE path is obstructed, while the RIS provides an alternative two-hop propagation route by redirecting the incident signal toward the UE.

For an N-element uniform linear array with inter-element spacing d, the phase shift applied to each RIS element must be selected so that the reflected signal components combine coherently at the receiver. The required phase at element n is

International Journal of Engineering Research & Technology (IJERT)
ISSN: 2278-0181
Vol. 15 Issue 07 , July - 2026

determined by the relative phase progression of the incident and reflected wavefronts.

The phase required at the nth RIS element to coherently combine the incident and reflected wavefronts is given by the generalized reflection, or phase-gradient, condition:

$$\phi_n = -k_0\, d\, n\, (\sin\theta_{\text{in}} + \sin\theta_{\text{out}}) \pmod{2\pi} \tag{1}$$

where $k_0 = 2\pi/\lambda$ is the free-space wavenumber, θ_{in} is the angle of incidence from the gNB, and θ_{out} is the angle of departure toward the UE. When the phase applied by every element satisfies (1), the reflected components add coherently at the receiver. Under ideal conditions, the corresponding array gain scales as $20\log_{10}(N)$ dB [3].

In practice, however, θ_{out} must be estimated because the exact UE position and the channel's angular parameters are not known a priori. An error in the estimated departure angle therefore produces a phase error at each RIS element. Since the phase term in (1) increases with the element index n, the resulting error accumulates across the surface, making elements farther from the array reference point more sensitive to angular-estimation inaccuracies than elements near the centre.

This behaviour highlights a fundamental engineering trade-off in RIS design. Increasing the number of reflecting elements provides a higher potential array gain, but it also imposes progressively stricter requirements on CSI and angular-estimation accuracy. Consequently, the theoretical gain of a large RIS can only be realised when its phase profile is configured with sufficiently precise channel information.

IV. Theoretical Background

A. mmWave Blockage and RIS-Assisted Propagation

At mmWave frequencies, a single obstruction, such as a wall, vehicle, or dense crowd, can introduce sufficient attenuation to reduce an otherwise reliable line-of-sight link to an outage. Owing to the short wavelength, diffraction around obstacles is weak and therefore provides only limited support for maintaining connectivity.

An RIS panel positioned with line-of-sight visibility to both the gNB and the shadowed coverage area can transform such an outage into a controllable, although inherently lossy, two-hop reflected path. The resulting performance improvement depends primarily on two factors: the number of RIS elements that contribute coherently to the reflected signal and the accuracy with which the phase profile defined in (1) can be implemented under realistic channel-state-information conditions.

B. RIS Phase-Configuration Error Model

In this study, the gNB-to-RIS geometry is assumed to be fixed and accurately pre-calibrated. This assumption is reasonable because the link connects two stationary infrastructure points and can therefore be surveyed and configured with high precision during deployment.

In contrast, the RIS-to-UE departure angle, θ_{out}, must be estimated dynamically as the UE changes position. In practice,

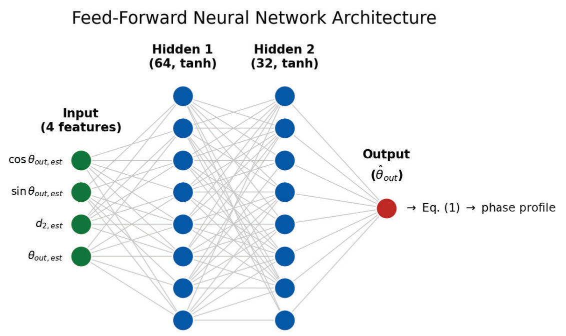

Fig. 2: Feed-forward neural-network architecture used for angle-of-departure correction. The model receives four input features, processes them through two hidden layers with hyperbolic tangent activation functions, and produces a single corrected angle estimate. This output is then substituted into the closed-form phase-gradient expression in (1) to reconstruct the RIS phase profile.

this estimate may be derived from uplink sounding measurements, localisation information, or a combination of both. These measurements are affected by multipath propagation, shadowing, measurement noise, and limitations in the angular-estimation process.

Rather than representing the angular error solely as independent additive Gaussian noise, this work introduces a nonlinear, position-dependent bias term together with a smaller residual Gaussian component. The nonlinear term is intended to capture systematic estimation errors that can arise from multipath-distorted angle-of-arrival and angle-of-departure measurements in practical environments.

This modelling choice is important to the methodology of the study. A purely unbiased Gaussian error model may be adequately corrected by a linear estimator and would therefore provide limited evidence for the benefit of a more expressive learning model. By introducing a genuine nonlinear bias structure, the comparison between linear regression and the proposed neural-network correction becomes more meaningful. It allows the evaluation to determine whether the neural network can learn and compensate for complex error patterns that cannot be fully represented by a linear mapping.

C. Machine-Learning Framework for Phase Correction

The phase-correction task is formulated as a supervised regression problem. The model receives the noisy estimate of the RIS-to-UE angle of departure together with a noisy estimate of the RIS-to-UE distance. The sine and cosine transformations of the estimated angle are also included as input features to avoid discontinuities caused by angular wrapping at the $-\pi$ and π boundaries.

Using these input features, the model predicts the true angle of departure, θ_{out}. The corrected angular estimate is then substituted into (1) to reconstruct the complete RIS phase profile across all reflecting elements. The resulting continuous phase values are subsequently quantised according to the supported hardware phase resolution before being applied to the RIS.

International Journal of Engineering Research & Technology (IJERT)
ISSN: 2278-0181
Vol. 15 Issue 07 , July - 2026

The reconstructed phase profile is quantised according to the resolution supported by the RIS hardware. Three configurations are considered: 1-bit, 2-bit, and 3-bit phase control, corresponding to 2, 4, and 8 discrete phase states per element, respectively. These configurations are consistent with practical PIN-diode-based RIS implementations and the discrete phase-shift model described in [8].

A feed-forward neural network with two hidden layers and hyperbolic tangent activation functions is trained using the designated training subset and evaluated on previously unseen test samples. Its performance is compared against two reference methods: an uncorrected baseline, in which the noisy angle estimate is used directly, and a linear-regression baseline trained using the same input features. The linear model is included specifically to determine whether the nonlinear representation learned by the neural network provides a measurable advantage.

Fig. 2 summarizes the proposed architecture. Importantly, the neural network does not estimate the RIS phase profile directly. Instead, it predicts a single corrected angle of departure, which is then substituted into the same closed-form geometric relationship in (1) used by the uncorrected and linear-regression baselines. This design ensures a fair comparison among the three approaches, since they share the same downstream phase-generation and quantization process and differ only in the accuracy of the angle estimate supplied to it.

V. Study Objectives

A. Evaluation of Practical Feasibility

The primary objective of this study is to quantify the proportion of the theoretical RIS beamforming gain that can be retained under realistic angle-of-departure estimation errors. The study further investigates whether a learning-based correction method can recover a meaningful portion of the gain lost because of inaccurate angular information.

B. Measurement of Key Performance Indicators

The evaluation focuses on two principal performance indicators. The first is the achieved beamforming gain relative to the ideal phase-error-free configuration, which represents the upper performance limit of the RIS-assisted link. The second is the angle-estimation error, measured by comparing the estimated or corrected angle of departure with its true value.

Together, these indicators provide a direct assessment of both estimation accuracy and its resulting impact on RIS performance. Angle error reflects the effectiveness of each correction strategy at the parameter-estimation level, while relative beamforming gain shows whether the improved estimate translates into a practical enhancement in coherent signal combining. The angle-estimation root-mean-square error (RMSE) is evaluated across three RIS phase-shifter quantisation resolutions.

C. Validation of Theoretical Predictions

The ideal quantization-only loss is calculated analytically and used as an upper-bound reference. The performance of the uncorrected, linear-regression-corrected, and neural-network-corrected methods is then compared against this benchmark. The linear-regression model is included as an important reference case to determine whether the improved representational capability of the neural network produces a genuine performance advantage. This comparison helps establish whether the additional model complexity is justified by measurable improvements in angular accuracy and beamforming gain.

D. Identification of Operational Challenges

This study investigates the effect of systematic estimation bias, in addition to random estimation variance, on RIS-assisted beamforming performance. Particular attention is given to the sensitivity of large RIS arrays to angular error, since the phase error at each element increases with its position relative to the array reference point. As a result, small angular inaccuracies can create substantial phase deviations at the outer elements of the array, reducing coherent combining and limiting the practical gain of larger RIS panels.

E. Development of Practical Guidelines

A further objective is to identify the operating conditions under which a learned correction method provides sufficient performance improvement to justify its added computational complexity relative to a simpler linear-regression approach. The study also evaluates how this benefit varies across different phase-quantisation resolutions and determines the hardware configurations for which nonlinear correction provides the greatest practical value.

VI. Simulation Setup and Modelled Configuration

A. Test Environment

The modelled scenario consists of a fixed gNB and a fixed RIS panel mounted at the corner of a building. The RIS is positioned 40 m from the gNB, with a clear line-of-sight path between the two infrastructure nodes.

UEs are randomly distributed within a two-dimensional region extending approximately 45–90 m from the gNB along one axis and 10–60 m along the perpendicular axis. This region represents an obstacle-dense environment, such as an urban plaza, courtyard, or mass-gathering venue.

The direct gNB-to-UE line-of-sight path is assumed to be blocked throughout the target region. Consequently, the UEs can receive the mmWave signal only through the two-hop gNB-to-RIS-to-UE reflected path.

B. Equipment and Configuration

The simulated system operates at 26 GHz and employs a 64-element uniform linear RIS array with half-wavelength element spacing. The gNB-to-RIS link is assumed to be fixed and accurately pre-calibrated, while the RIS-to-UE geometry varies according to the randomly generated UE positions.

International Journal of Engineering Research & Technology (IJERT)
ISSN: 2278-0181
Vol. 15 Issue 07 , July - 2026

TABLE I: Simulation Configuration

Parameter	Specification
Operating frequency	26 GHz mmWave
RIS array	64-element uniform linear array
Element spacing	$\lambda/2$
Phase resolution	1-, 2-, and 3-bit
gNB-to-RIS distance	40 m, fixed and pre-calibrated
RIS-to-UE distance	10–70 m, randomly generated
AoD-estimation error	Nonlinear bias with Gaussian noise
Distance-estimation error	Gaussian, $\sigma = 0.8$ m
Machine-learning model	Feed-forward NN, two hidden layers
Baseline methods	Uncorrected estimate, linear regression
Dataset size	8,000 samples, 75/25 train/test split

The RIS elements are evaluated using 1-bit, 2-bit, and 3-bit phase-control resolutions, corresponding to 2, 4, and 8 available phase states per element, respectively. This enables the study to assess the interaction between angle-estimation accuracy, machine-learning-based correction, and practical hardware quantization.

VII. Data and Methodology

All results presented in Section VIII were obtained through simulation rather than measurements from a physical RIS deployment. The dataset was generated using the system geometry, channel assumptions, estimation-error model, and hardware configurations described in the preceding sections. The simulation dataset was constructed according to the following procedure:

1) UE positions are generated uniformly at random within the NLoS region defined in Section VI-A. For each position, the true angle of departure, θ_{out}, and the true RIS-to-UE distance, d_2, are calculated directly from the known geometry. The corresponding ideal RIS phase profile is then obtained using (1).

2) Realistic estimation errors are applied to the geometric parameters. The angle-of-departure estimate is corrupted by a nonlinear, position-dependent bias representing systematic multipath-induced error, together with a smaller zero-mean Gaussian component having a standard deviation of $1.5°$. The RIS-to-UE distance estimate is independently perturbed by zero-mean Gaussian noise with a standard deviation of 0.8 m.

3) Three phase-configuration strategies are derived from the resulting noisy information. In the first, referred to as the naive strategy, the noisy angle estimate is substituted directly into (1) without correction. In the second, a linear-regression model is trained to predict the true departure angle from the noisy input features. This model serves as a low-complexity baseline for determining whether a simple linear correction can recover most of the achievable performance.

The third strategy uses a feed-forward neural network trained on the same input features and training split as the linear-regression model. This neural network constitutes the proposed phase-correction method evaluated in this paper.

Fig. 3 presents the neural-network training-loss curve. The mean-squared error converges within approximately 60 epochs under the early-stopping criterion, with no evidence of instability or divergence during training.

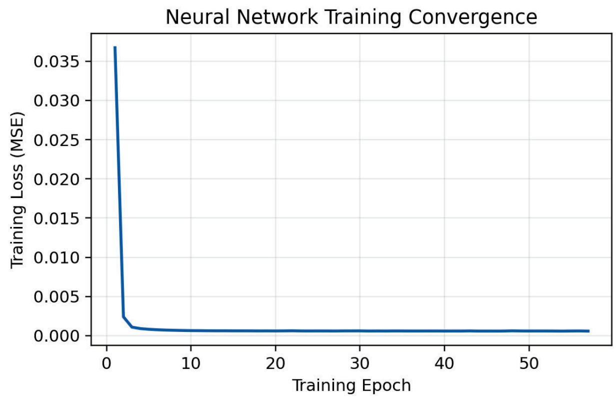

Fig. 3: Neural-network training convergence, shown as mean-squared error versus training epoch, with early stopping applied to prevent overfitting.

TABLE II: Achieved Beamforming Gain by Strategy and Quantisation (dB relative to ideal coherent combining)

Strategy	1-bit	2-bit	3-bit
Ideal CSI (quant. only)	-3.85	-0.89	-0.22
Naive (uncorrected)	-22.19	-20.31	-20.13
Linear-corrected	-11.48	-8.67	-8.16
NN-corrected	-11.03	-8.25	-7.70

4) The three phase-configuration strategies, together with the noise-free ideal case, are evaluated using a held-out test set comprising 25% of the dataset. These samples are not used during model training. For each test sample, the resulting phase profile is quantized to 1-bit, 2-bit, and 3-bit resolution. The corresponding array-factor gain is then calculated relative to the ideal coherent-combining condition.

Accordingly, the dataset and all beamforming-gain values reported in this study are simulation outputs produced using a physically grounded phase-error model. They are not measurements obtained from a live RIS deployment. Section IX discusses the additional experimental procedures and hardware requirements needed to validate the simulation results in a practical RIS test environment.

VIII. Results and Analysis

A. Modelled Key Performance Indicators

Table II presents the mean beamforming gain achieved by each phase-configuration strategy across the three phase-quantization resolutions. All values are expressed relative to the ideal noise-free coherent-combining condition. On the held-out test set, the angle-estimation RMSE was $6.01°$ for the uncorrected estimate, $1.95°$ after linear-regression correction, and $1.83°$ after neural-network correction.

Fig. 4 illustrates the corresponding beamforming-gain comparison. The uncorrected strategy incurs a loss of approximately 20 dB relative to the ideal case across all three quantization levels. This level of degradation removes most of the gain expected from a 64-element RIS and demonstrates the severe sensitivity of coherent combining to angular-estimation error.

International Journal of Engineering Research & Technology (IJERT)
ISSN: 2278-0181
Vol. 15 Issue 07 , July - 2026

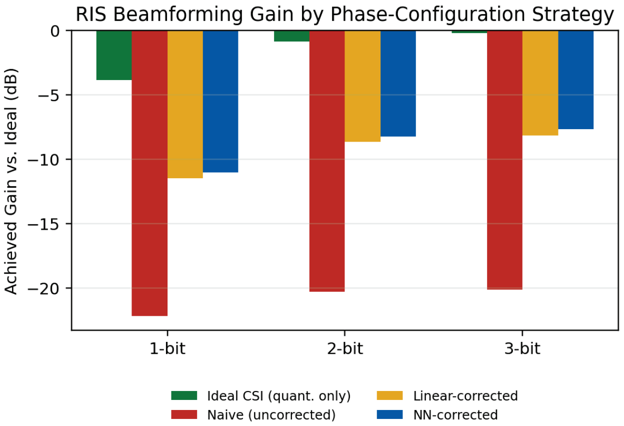

Fig. 4: Achieved RIS beamforming gain relative to ideal coherent combining for the uncorrected, linear-regression-corrected, and neural-network-corrected phase-configuration strategies under 1-bit, 2-bit, and 3-bit hardware quantization.

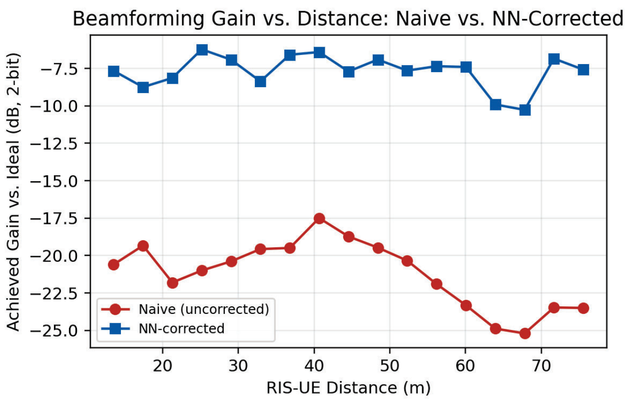

Fig. 5: Achieved RIS beamforming gain at 2-bit phase quantization as a function of RIS-to-UE distance, comparing the uncorrected phase-configuration strategy with the neural-network-corrected approach.

Both correction methods recover a substantial proportion of the lost beamforming gain. The neural-network model consistently outperforms the linear-regression baseline, although the improvement is moderate because the linear model already corrects a large part of the systematic estimation error. The advantage of the neural network is most visible at 1-bit phase resolution, where the residual loss is 11.03 dB compared with the corresponding loss obtained using linear correction. At 1-bit phase resolution, the neural-network-corrected strategy incurs a residual loss of 11.03 dB, compared with 11.48 dB for the linear-regression baseline. The improvement is relatively small because coarse phase quantization limits how accurately either correction method can reproduce the desired continuous phase profile.

B. Trend Analysis

Fig. 5 presents the achieved beamforming gain as a function of RIS-to-UE distance for the naive and neural-network-corrected strategies under 2-bit phase quantization. The naive method exhibits substantial gain degradation across the entire distance range because the position-dependent angular bias

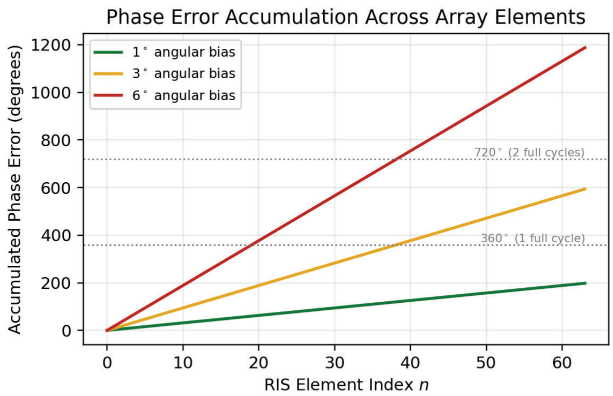

Fig. 6: Accumulated phase error across the RIS element index for representative angular-bias values, demonstrating that phase error increases with element position and causes the outer elements of larger arrays to decorrelate first.

remains present and does not diminish as the UE moves farther from the RIS.

In contrast, the neural-network-corrected strategy maintains a considerably smaller and more stable gap relative to the ideal case throughout the evaluated region. This behavior indicates that the learned correction generalizes across the tested geometry rather than merely fitting a limited subset of UE positions or distances.

IX. Discussion

A. Theoretical and Practical Alignment

The approximately 20 dB loss observed with the naive strategy is consistent with the phase relationship defined in Eq. (1). Because the phase error increases linearly with the element index n, even a small angular estimation bias can produce a large cumulative phase deviation across a 64-element array. At the outer elements, this deviation may span several multiples of 2π, causing the reflected signals to lose coherence and significantly reducing the achievable array gain.

Fig. 6 illustrates this effect more clearly. With an angular bias of only $3°$, the accumulated phase error exceeds a complete $360°$ cycle by approximately the midpoint of the array, and exceeds two complete cycles at the far edge. As a result, the contributions from the outer elements become effectively misaligned with the intended reflection direction and no longer combine coherently. This explains why seemingly small errors in the estimated UE direction can lead to a substantial degradation in received power, particularly for large RIS configurations. This behavior is consistent with the broader findings reported in the RIS literature [3], [4], where larger arrays are shown to be increasingly sensitive to channel-state information and angular-estimation accuracy. The results therefore confirm that some form of phase-correction mechanism is essential when a moderately sized RIS operates using estimated rather than perfectly known angular information.

B. System Limitations

This work is based on simulation and does not constitute hardware-level validation. The bias model used to represent

International Journal of Engineering Research & Technology (IJERT)
ISSN: 2278-0181
Vol. 15 Issue 07 , July - 2026

multipath-induced angular-estimation errors is intentionally simplified and illustrative rather than calibrated using measurements from a specific propagation environment. Consequently, a different error distribution or spatial bias pattern could produce better or worse performance for the linear correction baseline than that reported here.

The model also does not account for mutual coupling between neighboring RIS elements, which can alter the amplitude and phase response of practical arrays. Other implementation effects, including phase-quantization errors, element-to-element variations, finite reflection efficiency, control latency, hardware losses, and imperfect array calibration, are also excluded. These factors may reduce the absolute gains achievable in a real deployment.

In addition, the study assumes a simplified propagation geometry and a relatively stable channel during the optimization process. In practical mobile environments, user movement, time-varying blockage, diffuse scattering, and rapidly changing channel conditions may require more frequent phase updates and could increase the computational and signaling overhead. The reported results should therefore be interpreted as evidence of the proposed method's potential under controlled conditions rather than as a direct prediction of field performance.

The model also excludes mutual coupling between RIS elements, which can significantly affect the behaviour of large arrays [10]. In addition, the comparison assumes that the gNB-RIS segment is perfectly calibrated. This assumption is reasonable when the first hop behaves as a fixed, backhaul-like link, but it would need to be reconsidered in scenarios where the gNB, RIS, or surrounding propagation environment is mobile or dynamically reconfigured.

C. Deployment Implications

The main practical implication is that the structure of the estimation error is as important as its magnitude when selecting an appropriate correction method. If the error is approximately unbiased and follows a predominantly linear relationship with the raw measurements, a lightweight linear correction may recover most of the available performance improvement with minimal computational overhead. This is particularly valuable in mobile scenarios, where RIS phase profiles must be updated within the limited channel coherence time of a moving UE.

When the estimation error contains meaningful nonlinear characteristics, as represented in this study, a trained nonlinear model can provide an additional performance margin. Although this improvement is relatively modest, it remains practically relevant, particularly under coarse phase quantization. The benefit is most pronounced for 1-bit RIS configurations, which are among the most likely architectures for low-cost commercial deployment because of their reduced control complexity, lower power consumption, and simpler hardware implementation.

These findings suggest that correction complexity should be selected according to the expected error structure and hardware constraints. Linear correction may be sufficient for stable and well-characterized environments, whereas nonlinear learning-based correction may be more appropriate in propagation conditions affected by complex multipath, blockage, or systematic estimation bias.

D. Potential Improvements

Several extensions could improve the realism and general applicability of the proposed framework. First, explicitly modelling mutual coupling between RIS elements [10] would provide a more accurate representation of large-array behavior and practical element interactions. Second, replacing the stylized angular-bias model with an error pattern derived from measured or ray-traced channel data would allow the correction methods to be evaluated under more representative propagation conditions.

The framework could also be extended to reduced-CSI or implicit-CSI training approaches [12], thereby decreasing the channel-estimation and signaling burden associated with RIS configuration. This would be particularly relevant for mobile deployments, where frequent acquisition of complete CSI may be impractical.

Finally, integrating the proposed phase-correction approach with the coverage-enhancement perspective adopted in passive-reflector studies [9] would support a more complete end-to-end link-budget analysis. Such an extension could translate the beamforming gains reported in this study into system-level performance indicators, including achievable throughput, spectral efficiency, coverage probability, and outage probability. Hardware validation using a practical RIS prototype would represent the most important next step for confirming whether the observed simulation gains can be maintained under realistic quantization, calibration, coupling, and control constraints.

X. Conclusion

The gap between a 64-element RIS's theoretical promise and what it actually delivers comes down almost entirely to one thing: how well the phase profile matches the real angles involved. Get the angle-of-departure estimate wrong by even a few degrees, and the loss compounds across the array until roughly 20 dB of achievable gain simply disappears. A plain linear correction claws back most of that. A trained neural network claws back a bit more on top, and the edge it provides is largest exactly where cheap RIS hardware is most limited, at 1-bit phase resolution. So the honest takeaway is a modest one: machine learning helps here, but it is not what makes RIS viable in the first place, a much simpler correction already does most of the work. That is a useful thing to know before investing in a more complex model than the problem actually needs. Within Saudi Arabia's Vision 2030 push for resilient digital infrastructure [1], RIS is an attractive way to extend mmWave coverage into obstacle-dense areas without a matching increase in small-cell count, provided this phase-error problem is dealt with somehow. What this paper cannot yet answer is whether the specific bias pattern assumed

International Journal of Engineering Research & Technology (IJERT)
ISSN: 2278-0181
Vol. 15 Issue 07 , July - 2026

here matches what real hardware would see. The remaining validation gap, together with accurate modelling of mutual coupling between RIS elements, represents the most important direction for future work.

Acknowledgment

All research design decisions, modelling assumptions, simulation procedures, and analytical interpretations were developed and verified by the authors. AI-assisted tools were used solely to support language refinement, simulation-code organization, and document formatting. The authors retained full responsibility for the technical content, validation, and conclusions presented in this paper.

References

[1] Kingdom of Saudi Arabia, "Saudi Vision 2030." [Online]. Available: https://www.vision2030.gov.sa
[2] 3GPP, "Study on channel model for frequencies from 0.5 to 100 GHz," 3GPP TR 38.901, ver. 16.1.0, 2019.
[3] W. Tang, X. Chen, M. Z. Chen, J. Y. Dai, Y. Han, M. Di Renzo, S. Jin, Q. Cheng, and T. J. Cui, "Path loss modeling and measurements for reconfigurable intelligent surfaces in the millimeter-wave frequency band," *IEEE Trans. Commun.*, vol. 70, no. 9, pp. 6259–6276, Sep. 2022.
[4] F. H. Danufane, M. Di Renzo, J. de Rosny, and S. Tretyakov, "On the path-loss of reconfigurable intelligent surfaces: An approach based on Green's theorem applied to vector fields," *IEEE Trans. Commun.*, vol. 69, no. 8, pp. 5573–5592, Aug. 2021.
[5] Q. Wu and R. Zhang, "Towards smart and reconfigurable environment: Intelligent reflecting surface aided wireless network," *IEEE Commun. Mag.*, vol. 58, no. 1, pp. 106–112, Jan. 2020.
[6] M. Di Renzo, A. Zappone, M. Debbah, M.-S. Alouini, C. Yuen, J. de Rosny, and S. Tretyakov, "Smart radio environments empowered by reconfigurable intelligent surfaces: How it works, state of research, and the road ahead," *IEEE J. Sel. Areas Commun.*, vol. 38, no. 11, pp. 2450–2525, Nov. 2020.
[7] E. Basar, M. Di Renzo, J. de Rosny, M. Debbah, M.-S. Alouini, and R. Zhang, "Wireless communications through reconfigurable intelligent surfaces," *IEEE Access*, vol. 7, pp. 116753–116773, Aug. 2019.
[8] Q. Wu and R. Zhang, "Beamforming optimization for wireless network aided by intelligent reflecting surface with discrete phase shifts," *IEEE Trans. Commun.*, vol. 68, no. 3, pp. 1838–1851, Mar. 2020.
[9] W. Khawaja, O. Ozdemir, Y. Yapici, F. Erden, and I. Guvenc, "Coverage enhancement for NLOS mmWave links using passive reflectors," *IEEE Open J. Commun. Soc.*, vol. 1, pp. 263–281, Jan. 2020.
[10] B. Peng, K.-L. Besser, S. Shen, F. Siegismund-Poschmann, R. Raghunath, D. Mittleman, V. Jamali, and E. A. Jorswieck, "RISnet: A domain-knowledge-driven neural network architecture for RIS optimization with mutual coupling and partial CSI," *IEEE Trans. Wireless Commun.*, vol. 24, no. 5, pp. 4469–4482, May 2025.
[11] Ö. Özdogan and E. Björnson, "Deep learning-based phase reconfiguration for intelligent reflecting surfaces," in *Proc. 54th Asilomar Conf. Signals, Systems, and Computers*, 2020, pp. 707–711.
[12] T. Jiang, H. V. Cheng, and W. Yu, "Learning to reflect and to beamform for intelligent reflecting surface with implicit channel estimation," *IEEE J. Sel. Areas Commun.*, vol. 39, no. 7, pp. 1931–1945, Jul. 2021.
[13] P. Fondo-Ferreiro, F. B. Saghezchi, F. Gil-Castiñeira, and J. Rodriguez, "Neural networks for phase-shift optimization of reconfigurable intelligent surfaces under imperfect channel state information," *IEEE Access*, vol. 13, pp. 53694–53705, 2025.
[14] Z. Li, S. Wang, Q. Lin, Y. Li, M. Wen, Y.-C. Wu, and H. V. Poor, "Phase shift design in RIS-empowered wireless networks: From optimization to AI-based methods," arXiv:2204.13372, 2022.
[15] T. L. Marzetta, "Noncooperative cellular wireless with unlimited numbers of base station antennas," *IEEE Trans. Wireless Commun.*, vol. 9, no. 11, pp. 3590–3600, Nov. 2010.
[16] C. E. Shannon, "A mathematical theory of communication," *Bell Syst. Tech. J.*, vol. 27, no. 3, pp. 379–423, Jul. 1948.
[17] 3GPP, "NR; User Equipment (UE) radio transmission and reception; Part 2: Range 2 standalone," 3GPP TS 38.101-2.